communications earth & environment

Article

A Nature Portfolio journal

https://doi.org/10.1038/s43247-026-03334-0

High-enthalpy Larderello geothermal system, Italy, powered by thousands of cubic kilometres of mid-crustal magma

Check for updates

Matteo Lupi[1], Douglas Stumpp[1], Iván Cabrera-Pérez[1], Konstantinos Michailos[1,2], Gilberto Saccorotti[3], Marco Bonini[4], Federico Farina[5], Elliot Amir Jiwani-Brown[1], Riccardo Lanari[4], Samuele Papeschi[4], Geneviève Savard[1], Juan Porras[1], Julien Sfalcin[6], Francisco Muñoz-Burbano[1], Riccardo Minetto[7], Chiara Del Ventisette[8], Davide Piccinini[3] & Domenico Montanari[4]

Thousands of cubic kilometers of magma lie in the upper crust below supervolcanoes such as Yellowstone (USA), Toba (Indonesia), and Taupo (New Zealand). Most of these systems are identified because of surface geomorphology and eruptive deposits. Recognizing such volcanoes without surface evidence is challenging, causing large magmatic reservoirs to go unnoticed. The Tuscan Magmatic Province, Italy, features only sparse Quaternary volcanic activity, but subsurface data indicate the presence of supercritical fluids at shallow depths. Here we show that more than 5'000 km^3 of magma and partial melt are stored in the middle crust of the Tuscan Magmatic Province, Italy. This fuels the high-enthalpy geothermal systems of the region. Such volumes are comparable to those of mid-crust reservoirs beneath recognized supervolcanoes. The discovery of large volumes of magma is critical to explain the long-term evolution of mature magmatic systems and to understand the behavior of large magmatic provinces.

In continental regions, large reservoirs of highly viscous partial melt can be stored in the crust[1,2]. Their surface expression consists of subsidence-driven caldera-like morphology, which can extend over 100 km^2 (or more). Such systems have generated massive and catastrophic eruptions, producing thousands of cubic kilometers of volcanic material (e.g., Yellowstone and Long Valley in the USA, Toba in Indonesia)[3]. These deposits are thought to result from magmas that ascend from the upper mantle into the crust[4,5]. These deep reservoirs feed shallower, sub-horizontal reservoirs in the middle crust, which can extend for dozens of kilometers in diameter[5–9].

The western coast of Italy is marked by volcanic systems that in the past have produced VEI 7 eruptions, like the Colli Albani[10] or the currently inflating Campi Flegrei caldera[11,12]. Further North, in a similar geodynamic setting, lies the Tuscan Magmatic Province (TMP) featuring small-sized silicic shallow-level plutons[13] and volcanic products, but where no major Holocene eruptions have been identified (the most recent eruptions are those of the Mt. Amiata about 300-200 ka[14]). The lack of volcanic eruptive features does not reconcile the subsurface data of the Larderello-Travale geothermal system (LTS), indicating an extreme heat flow locally reaching up to 1000 mWm^{-2}[15] (Fig. 1). This causes a geothermal gradient reaching more than 150 °C km^{-1}, intense microseismicity and the suggested occurrence of super-critical fluids at shallow depths[16] with temperatures that locally exceed 500°C at about 3 km depth[16].

The presence of magma at depth has been postulated for the LTS, but boreholes[17], active seismic profiles[18], gravimetric[19], electromagnetic[20], passive seismic imaging[21,22], and low-temperature thermochronology[23] data have not provided a definitive answer (so far). However, active seismic acquisitions speculate the occurrence of intrusions at about 10 km depth[24]. Unfortunately, previous passive seismic imaging studies in southern Tuscany have either covered large areas with sparse seismic networks[25–28] or focused on small regions with dense seismic deployments[21,22,29]. This resulted in incomplete imaging of the geothermal system, in particular its deeper feeding regions. We deployed a network of 30 broadband seismometers from September 2020 to September 2021 to integrate the publicly permanent Italian (INGV) seismic network (Fig. 1) and process the data to perform an Ambient Noise Tomography (ANT)[30,31]. We used more than 60 broadband seismometers (see Fig. 1) to reconstruct the velocity structure of

[1]Department of Earth Sciences, University of Geneva, Geneva, Switzerland. [2]Research School of Earth Sciences, Australian National University, Canberra, ACT, Australia. [3]Istituto Nazionale di Geofisica e Vulcanologia, Pisa, Italy. [4]Institute of Geosciences and Earth Resources, National Research Council of Italy (CNR), Florence, Italy. [5]Department of Earth Sciences "A. Desio", Università degli Studi di Milano, Milano, Italy. [6]Invert SA, Canton Vaud, Switzerland. [7]Institut Terre et Environnement de Strasbourg, Université de Strasbourg/CNRS, Strasbourg, France. [8]Department of Earth Science, University of Florence, Florence, Italy.
e-mail: matteo.lupi@unige.ch; ivan.cabrera-perez@unige.ch

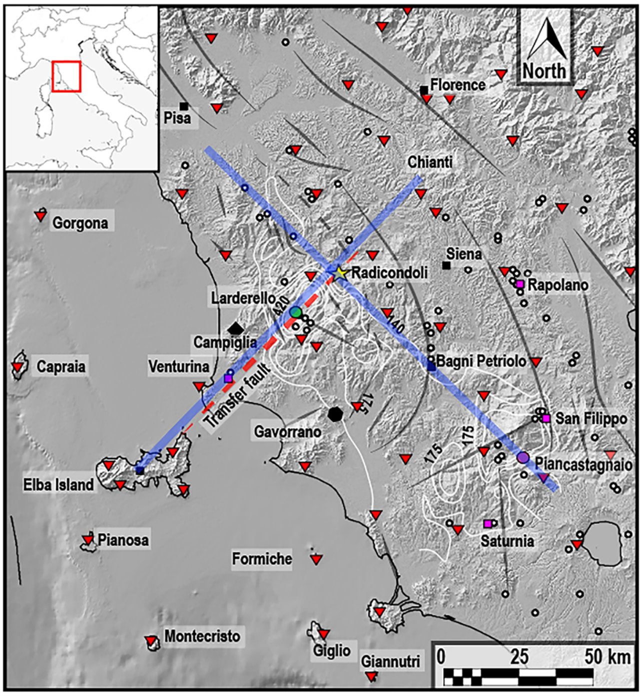

Fig. 1 | Map showing the spatial distribution of the seismic networks used in this study, which comprises 63 seismic sites (red triangles) in total. The network implements the stations of the INGV, RSNI, AASN, and RESIF networks with temporary stations. The major geothermal centers of Larderello, Radicondoli and Piancastagnaio are shown by the green circle, yellow star and pink circle, respectively. The white contour lines show the heat flow of the region that reaches peaks of extreme heat flow (up to 1000 mWm^{-2})[15] in the Larderello region. White circles show the distribution of main hydrothermal springs, and the black lines indicate the strikes of major regional faults. The inset map shows the location of the study area within Italy. The dashed red line indicates the strike of the inferred transfer zone[73]. The blue lines indicate the strikes of the cross-sections shown in Fig. 3.

the middle to upper crust of southern Tuscany. Then, we applied the ANT workflow to obtain the 3-D S-wave velocity model. This consists in the pre-processing of ambient noise signals, cross-correlation of ambient noise for pair of stations, extraction of dispersion curves for each pair, and generation of 2-D group velocity maps for different periods using a regularized linear least-square inversion approach[31–33]. Finally, we perform a 1-D depth inversion using a McMC transdimensional Bayesian inversion approach[34,35]. Details about the methodology are fully described in the supplementary online material.

Results

We obtained a 3-D shear wave velocity (V_s) model of the upper 15 km of the crust of Tuscany. We plot absolute and relative velocity variations across our model (Figs. 2, 3). To compute the anomaly maps, we use the 1-D reference model that is defined as the average V_s profile at each depth, calculated from the ambient noise model. For each depth, all V_s values are extracted and averaged to create the background model. Relative V_s variations are then computed as percentage deviations from this mean. The absolute and relative seismic velocities (Fig. 2) show transitions between fast and slow domains. At about 3 km depth the fast anomalies broadly fit the Tuscan metalliferous region[36,37] (e.g., centered around Gavorrano). This NW-striking fast body departs from Venturina and flanks the Tyrrhenian coast reaching about the Southern limit of our model. From Venturina, such a fast body seems to reach the eastern margin of Elba Island. Interestingly, the surface expressions of the hydrothermal centres, often coincide to a transition zone between fast and slow anomalies (e.g., Venturina, Larderello, Rapolano and Bagni di Petriolo in Fig. 2). The NE-striking transition between faster and slower bodies departing from Eastern Elba and reaching Larderello and even Radicondoli, fits surprisingly well the direction of postulated transfer faults[38] that are proposed to accommodate deformation in the region (Fig. 1).

At increasing depth (Fig. 2, 8 km depth) the NW-striking fast body becomes more prominent. Its fastest domain mimics the surface expression of the TMP enriched in ore deposits[36]. In the central and Southeastern parts of our model, two low-shear-wave regions become more prominent. Both the geothermal fields of Larderello and Radicondoli seat on the shoulders of such a region. Similarly, the center of the Amiata geothermal field (i.e., Piancastagnaio) occurs at the limits of the low velocity domain in the South-East. These two slow-velocity zones are subelliptical in shape, with a minor axis striking between WNW and NNW (e.g., appenninic). At 12 km depth the regions are prominent, absolute shear wave velocities drop down to about 1.2 km/s at the core of such anomalies. The low-velocity zone becomes more diffuse towards the west and features a sharp transition into the fast units beneath the Gavorrano pluton.

The two vertical profiles (Fig. 3) cutting through some of the most relevant geological features show prominently low shear wave values lying below the major geothermal systems of Tuscany. In particular, along the NE-striking section, a sub-vertical domain of low V_s departs from the bottom of our inversion (conservatively cut at 15 km depth) and rises to about 8 km depth, below the LTS (Fig. 3). The SW margin of such an anomaly is sub-vertical in shape, and at about 10 km depth the contrast with most competent units is clear. On top of such a structure lies a region of (less-) slow shear waves compared to the surrounding regions. The perpendicular NW-striking cross-section cutting through the southern geothermal systems of Piancastagnaio-Amiata, shows that such a prominent low V_s region is not an isolated plume, but rather a widespread feature in the TMP. Instead, it is part of a particularly low shear wave domain that extends sub-horizontally southwards up to the Amiata geothermal system. Interestingly, the Mt Amiata, is the only volcano recognized in the region to have had activity during the Middle Pleistocene[39].

Discussion

We image in detail the seismic velocity structures of the upper 15 km of the crust in TMP. Resolution tests show that we can rely on inversions up to 15 km depth (see the supplemental online material, e.g. checkerboard (S9), kernels (S11), V_s uncertainty (S16)). The occurrence of cooling magmatic bodies in the middle crust of the TMP have been postulated in the past by several authors[24,40]. The comparison with available data seem to support the robustness of our inversion. The CROP-18A[24] runs sub-parallel to our NW-striking profile (Fig. 3). Its interpretation[24] indicates a transition zone between 3 to 4 km depth that we also detect. This region, named K-horizon[16,24,29,40], is a debated feature. Authors argue that it may represent either a tectonic[41] or a rheological boundary[29] or the accumulation of supercritical fluids at depth[40]. Our tomography contours and points out the extent of such a region. The K-horizon seem to be a transition zone enveloping the domain surrounding the sub-vertical low-velocity regions in the middle crust (Fig. 4).

With increasing depth, the velocity of shear waves is expected to increase in the continental crust. In geothermal and volcanic systems, this is often not the case because of the hydrothermal and magmatic fluids encountered at depth. We argue that the prominent reduction of shear waves shown in Figs. 2, 3, and 4 is related to the occurrence of magmatic fluids roofing up at about 3 km depth below the LTS. They roof at about 3 km depth where tourmaline indicating supercritical conditions have been found[13,42]. This is shown by the Venelle2 well drilled with the aim of penetrating the roof of the cupola shown in Fig. 4. At 2.8 km drilling encountered pressures and temperatures of 42.5 MPa and 512 °C, respectively[42]. The geothermal gradient increased sharply at 2750 m depth where the temperature was 380 °C[42]. According to the phase diagram of geothermal brines[43], under these conditions, fluids are found in a supercritical state. The occurrence of supercritical fluids at shallow depth implies that the intrusions speculated to occur at depth cannot be cold.

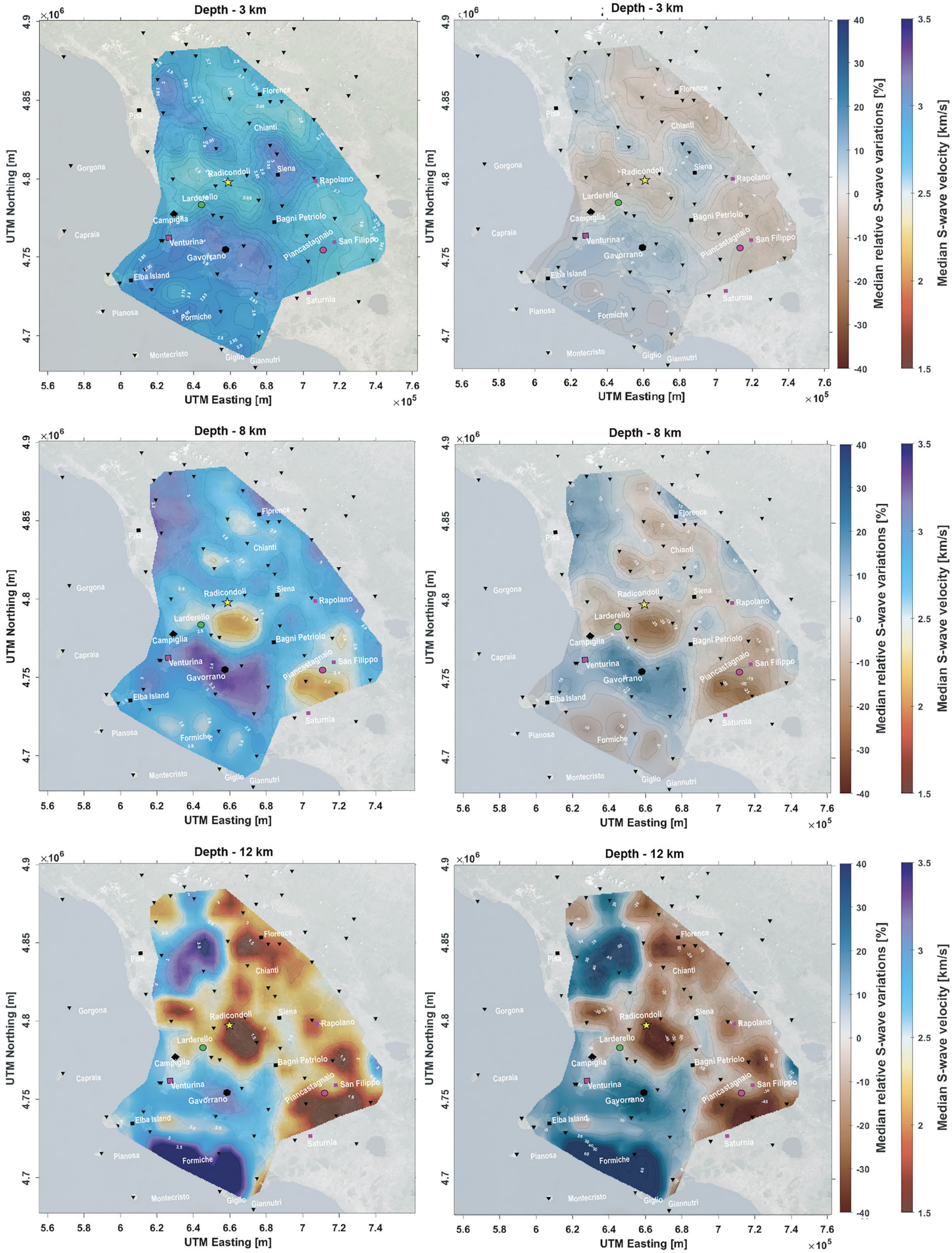

Fig. 2 | Shear-wave velocity and anomaly maps at different depths for the Tuscan Magmatic Province. Relative V_s variations are calculated by subtracting an average 1-D V_s depth profile of our model. Black triangles show the position of the seismic stations. The symbols are described in the caption of Fig. 1.

A vast literature reinforces the idea that magma is ponding somewhere in the upper crust of the TMP. The TMP is affected by an extremely high heat flow[15,17,42], gravity anomalies centered in Larderello[19] indicating denser material at depth, and by the widespread fumarolic activity that characterized this region (once called the Devil's Valley) before the onset of geothermal exploitation in the 19th century. The CROP-18 profile speculates about the potential occurrence of melts at about 10 km depth below LTS (but not below the Amiata volcano)[24]. Teleseismic receiver function studies point out a continuous pulse characterized by shear-wave velocities as low as 1.6 km s^{-1} that could be modelled with a dome-like structure across

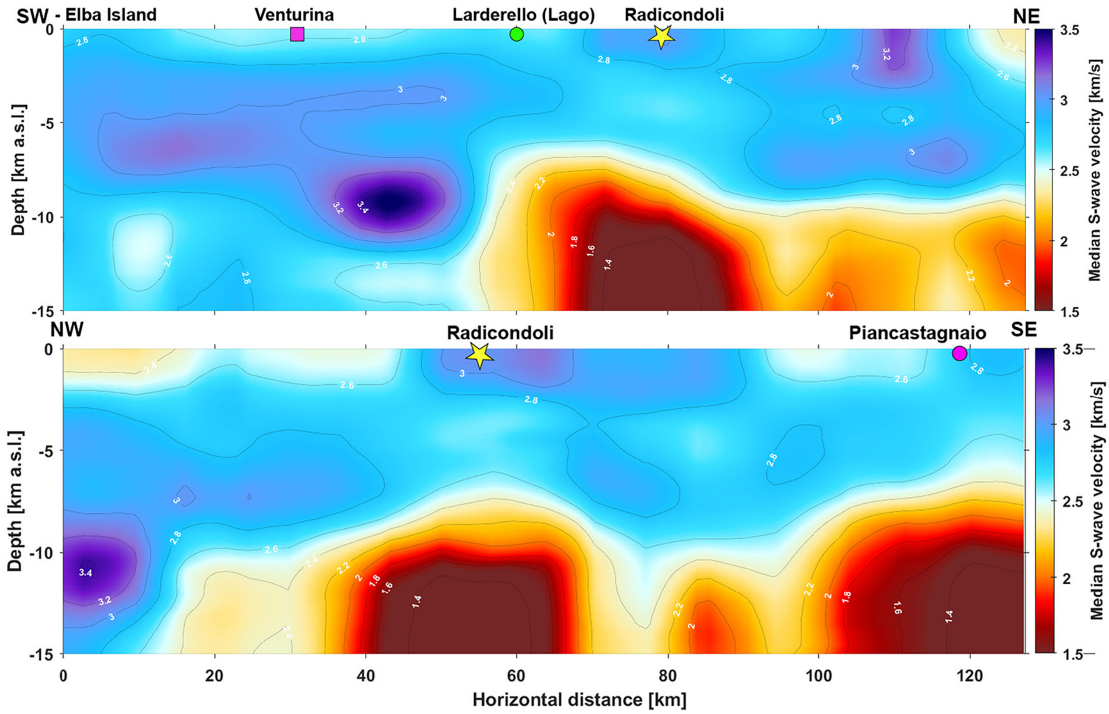

Fig. 3 | Absolute V_s cross-sections along the profiles shown in Fig. 1. The base of the lower crust highlights the widespread occurrence of slower Vs compared to the upper crust. The southern region (below Piancastagnaio - Mt. Amiata) also hosts large volumes of melt. Note that cross-sections are vertically exaggerated.

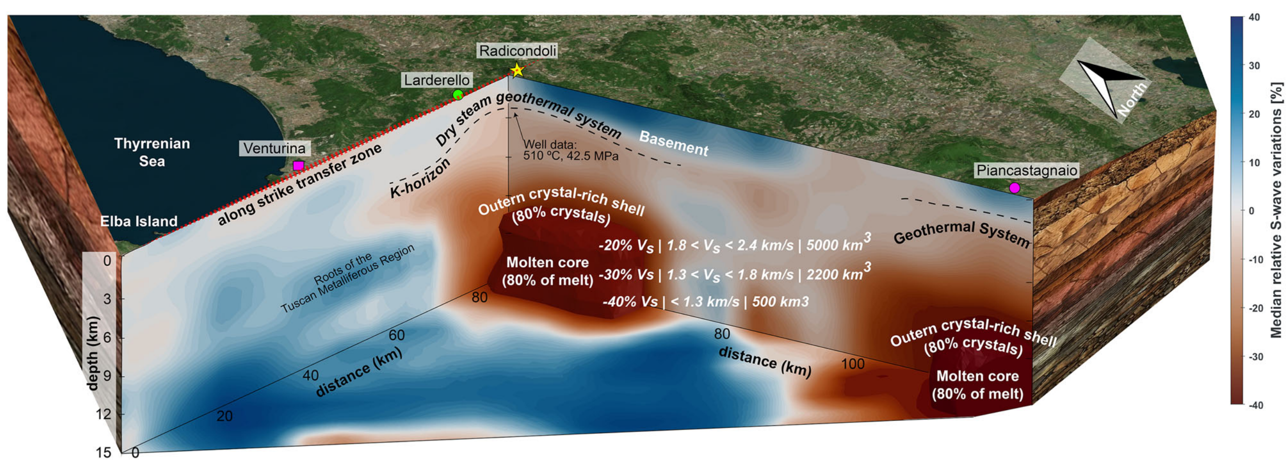

Fig. 4 | Conceptual model of the Tuscan Magmatic Province. The mid-crustal reservoirs are contoured based on a V_s anomaly value of -30%. The total calculated volumes for the magmas below Larderello is about 5000 km^3 plus a mush shell of an equally large volume surrounding the melt. Below the Piancastagnaio system, the volumes are estimated at least as large. However, the region falls at the margin of our model and should therefore be better assessed.

9–12 km depth[40]. Also, teleseismic V_p point out a reduction of about 18% in the middle crust below LTS, without being able to constrain the depth because of the long wavelength of the teleseismic waves[44].

Our inversion suggest the occurrence of V_s as low as 1.25 km s^{-1} at 10 km depth (Fig. 3). This corresponds to anomalies of about -40% (Fig. 4). Such low velocities are commonly attributed to the occurrence of magma or partial melt[45]. Constraints on the nature of the low-velocity zones are gained assuming they are constituted by a melt-saturated porous granite, for which melt fractions within the 20% - 40% interval are required to explain our extremely-low V_s values[46,47]. To shed light on the real nature of such low V_s values, we used MageMin[48]. The methods and the assumptions are described in the supplemental online material. To assess the fraction of melt that may cause the low V_s values shown in Figs. 2, 3, we define 3 regions corresponding to -40% ($V_s \leq 1.3$ km s^{-1}), -30% ($1.3 < V_s < 1.8$ km s^{-1}), and -20% ($1.8 \leq V_s \leq 2.4$ km s^{-1}). Results indicate that the low V_s region below Larderello shown in Fig. 3 has a core of melt with a liquid fraction higher than 80% and an outer crystal-rich region where the liquid fraction is about 20% of the total volume. This translates into about 3000 km^3 of partial melt surrounded by a region of about 5000 km^3 of crystal mush. The region below mount Amiata held even larger volumes (at least twice as large). However, the proximity to the limits of resolution of our model imposes a need for a more robust assessment of the melt volume in the region, possibly through additional seismic acquisitions. Additionally, our model is based on Rayleigh waves. Radial anisotropy is strongly positively anomalous in the plumbing systems of supervolcanoes because of the interlayered sill structure[49]. This may result in Love waves being faster than Rayleigh waves.

Our interpretation suggests large magmatic reservoirs in the middle crust is in line with previous studies investigating similar geological contexts, attributing such V_s magnitudes to the occurrence of melts[5,9,50–53]. Stratigraphic and morphological observations also suggest that these regions have

Table 1 | Summary of key parameters for five major magmatic systems

Volcanic system	Crustal reservoir volume (km^3)	Heat Flow (mWm^{-2}) or geothermal gradient (C°/km)	Vertical deformation	Largest Eruption (km^3)
Toba, ID	~ 34,000 (< 15 km)	~ 130[4]	At least 1.5 cm/yr[60] since 74 ky	2800 – 5300[60]
Taupō, NZ	200–1000 (5–8 km)[61]	~ 700[62]	Both subs. (tectonic) & uplift (magma migration)[63]	> 530[64]
Long Valley, USA	6400[56]	50 °C/km[65]	~ 0.8 m uplift (1975-2006)[66]	~ 600–650[67]
Yellowstone, USA	~ 10'000 (< 20 km)[5]	2000[68]	7 cm/yr uplift[69]	~ 850[70]
Campi Flegrei, IT	–	(400 °C at 3 km[71])	~ 1 m/yr uplift[72]	457–660[11]
LTS, IT	~ 5000	200–1000[15]	500 m uplift since Pliocene; 0,13 mm/yr[54]	*unknown*

LTS stands for Larderello-Travale geothermal system.

experienced an uplift in the order of 500 m because of the emplacement of granitic bodies in the upper crust[54].

The volumetric estimates of the melts in the TMP are of the same order of magnitude of those of some of the largest eruptive systems worldwide, such as Taupō, Long Valley, and Yellowstone[5,55,56]. All these volcanic systems featured super-eruptions. The literature excludes geological records of major eruptions released by vents hosted in Larderello or in the TMP. The 300 kya Amiata eruption only featured minor volumes eruptive volumes (10 km^3)[57] and the other eruptive centers did not produce any major volume.

The difference between a high-enthalpy geothermal and a volcanic system lies in the occurrence of at least one documented eruptive event and by an identified volcanic structure (i.e., cone or caldera). However, from a quantitative geophysical perspective, the plumbing system of a caldera (e.g. the Campi Flegrei) and the LTS are identical. They both share intense shallow seismic activity, vigorous fluid flow, gravity anomalies, fumarolic manifestations, and high heat flows resulting in extreme (volcano-like) geothermal gradients. Furthermore, compared with known supervolcanoes, the LTS features several parameters comparable to those of Yellowstone, Taupo, and other calderas. For instance, the heat flow measured at the LTS is comparable with the one measured in Yellowstone, while the volume of the crustal reservoir we identify (about 5000 km^3 for LTS) is comparable to the one mapped at the Long Valley caldera (Table 1). Yet, there is no recognised eruption associated with the LTS.

Despite no existing morphological evidence or Holocene volcanic eruptive products in the region hosting the LTS, we present evidence for the existence of large volumes of partial melt hosted in the upper crust of Tuscany. The reason why this large amount of melt never gave rise to eruptions is enigmatic and debated[58]. The volcanic systems of Latium that often erupted in the past are thought to be driven by the rise of a veined-metasomatized asthenospheric mantle wedge linked to the eastwards slab-rollback of the Adriatic plate[59]. The magmas of the Tuscan Magmatic Province are connected to the occurrence of peraluminous anatectic granitoids formed by crustal anatexis involving diverse metasedimentary sources in the Tuscan basement[13]. This geochemical characteristic may be a key aspect to consider when investigating the low eruptivity of the magmas shown in Fig. 4. The absence of significant eruptions fed by the large reservoir we image may result from the fertility of the middle-upper crust in Tuscany, linked to the composition of the magmas produced. Low-temperature, peraluminous magmas like those encountered in the wells of Larderello[13] are highly viscous, inhibiting eruptions. Such magmas may accumulate in the upper crust forming a viscous barrier hindering the ascent of melts. This process promotes top-down pluton formation through downwards accretion. The distribution of the shear wave velocities in our model indicates that such large partial melts feed a regional-scale fluid flow system upwelling to the surface at the boundaries of the low-velocity anomaly. This regional-scale fluid flow system may also explain the widespread occurrence of travertine deposits all over the southern portion of the Tuscan Magmatic Province as well as the extensive abundance of CO_2 in the region due to the metamorphic reactions promoted in the heated limestones.

Our study provides quantitative constraints and, for the first time, the size and location of magma in the middle crust of the Tuscan Magmatic Province, reconciling long-standing debates about the plumbing system of the LTS. Such partial melts may help understand the long-term evolutionary processes taking place at volcanic systems that featured super-eruptions and in regional-scale high-enthalpy systems that have not (yet?) erupted.

Data availability

The continuous seismic waveform data used in the present study are available at the European Integrated Data Archive (EIDA; http://www.orfeus-eu.org/data/eida/) with the following network codes: Z3 (AASN: https://doi.org/10.12686/ALPARRAY/Z3_2015); FR (RESIF and other broadband and accelerometric permanent networks in metropolitan France; https://doi.org/10.15778/RESIF.FR); IV (https://doi.org/10.13127/SD/X0FXNH7QFY); and GU (RSNI:https://doi.org/10.7914/SN/GU). The TEMPEST data are archived in the Incorporated Research Institutions for Seismology Data Management Center (IRIS–DMC) with network code 1K (https://www.fdsn.org/networks/detail/1K_2020).

Received: 28 July 2025; Accepted: 13 February 2026;
Published online: 14 April 2026

References

1. Bachmann, O. & Bergantz, G. The magma reservoirs that feed supereruptions. *Elements* **4**, 17–21 (2008).
2. Rasmussen, D. J., Plank, T. A., Roman, D. C. & Zimmer, M. M. Magmatic water content controls the pre-eruptive depth of arc magmas. *Science* **375**, 1169–1172 (2022).
3. Self, S.*Explosive Super-Eruptions and Potential Global Impacts*. M (Elsevier Inc., 2015). https://doi.org/10.1016/B978-0-12-396453-3.00016-2.
4. Jaxybulatov, K. et al. A large magmatic sill complex beneath the Toba caldera. *Science* **346**, 617–619 (2014).
5. Huang, H.-H. et al. The Yellowstone magmatic system from the mantle plume to the upper crust. *Science* **348**, 773–776 (2015).
6. Koulakov, I. & Shapiro, N. Seismic Tomography of Volcanoes. In *Encyclopedia of Earthquake Engineering*, 1–18 (Springer, 2021).
7. Gase, A. C. et al. Seismic evidence of magmatic rifting in the offshore Taupo volcanic zone, New Zealand. *Geophys. Res. Lett.* **46**, 12949–12957 (2019).
8. Shapiro, N. M. & Koulakov, I. Probing the underbelly of a supervolcano. *Science* **348**, 758–759 (2015).
9. Farrell, J., Smith, R. B., Husen, S. & Diehl, T. Tomography from 26 years of seismicity revealing that the spatial extent of the Yellowstone crustal magma reservoir extends well beyond the Yellowstone caldera. *Geophys. Res. Lett.* **41**, 3068–3073 (2014).
10. Giordano, G. & Team, T. C. Stratigraphy, volcano tectonics and evolution of the Colli Albani volcanic field https://doi.org/10.1144/IAVCEI003.4 (2010).

11. Silleni, A., Giordano, G., Isaia, R. & Ort, M. H. The Magnitude of the 39.8 ka Campanian Ignimbrite Eruption, Italy: method, uncertainties and errors. *Frontiers in Earth Science* **8**, 543399 (2020).
12. Vanorio, T., Geremia, D., De Landro, G. & Guo, T. The recurrence of geophysical manifestations at the campi flegrei caldera. *Sci. Adv.* **11**, eadt2067 (2025).
13. Farina, F. et al. Zircon petrochronology reveals the timescale and mechanism of anatectic magma formation. *Earth Planet. Sci. Lett.* **495**, 213–223 (2018).
14. Laurenzi, M. A., Braschi, E., Casalini, M. & Conticelli, S. New 40Ar-39Ar dating and revision of the geochronology of the Monte Amiata volcano, central Italy. *Ital. J. Geosci.* **134**, 255–265 (2015).
15. Mongelli, F. & Zito, G. Flusso di calore nella regione Toscana. *Studi Geologici Camerti Spec*. 91–98 (UNICAM, 1991).
16. Minetto, R. et al. Tectonic and anthropogenic microseismic activity while drilling toward supercritical conditions in the Larderello-Travale geothermal field, Italy. *J. Geophys. Res. Solid Earth* **125**, 1–17 (2020).
17. Romagnoli, P., Arias, A., Barelli, A., Cei, M. & Casini, M. An updated numerical model of the Larderello-Travale geothermal system, Italy. *Geothermics* **39**, 292–313 (2010).
18. Finetti, I. R. Basic regional crustal setting and superimposed local pluton-intrusion- related tectonics in the Larderello-M. Amiata geothermal province, from integrated CROP seismic data. *Boll. della Soc. Geologica Ital.* **125**, 117–146 (2006).
19. Orlando, L. Interpretation of Tuscan gravity data. *Boll. Della Soc. Geologica Ital., Suppl.* **3**, 179–186 (2005).
20. Santilano, A.*Deep geothermal exploration by means of electromagnetic methods: New insights from the Larderello geothermal field (Italy)*. Ph.D. thesis, (Politecnico di Torino, 2017).
21. De Matteis, R. et al. Three-dimensional tomography and rock properties of the Larderello-Travale geothermal area, Italy. *Phys. Earth Planet. Inter.* **168**, 37–48 (2008).
22. Bagagli, M., Kissling, E., Piccinini, D. & Saccorotti, G. Local earthquake tomography of the Larderello-Travale geothermal field. *Geothermics* **83**, 101731 (2020).
23. Montanari, D., Ruggieri, G., Bonini, M. & Balestrieri, M. L. First application of low temperature thermochronology as a tool for geothermal exploration: a promising, preliminary test from the Larderello-Travale geothermal field (Italy). *Geothermics* **107**, 102603 (2023).
24. Brogi, A. et al. Crustal structures in the geothermal areas of southern Tuscany (Italy): insights from the CROP 18 deep seismic reflection lines. *J. Volcanol. Geotherm. Res.* **148**, 60–80 (2005).
25. Di Stefano, R., Kissling, E., Chiarabba, C., Amato, A. & Giardini, D. Shallow subduction beneath Italy: Three-dimensional images of the Adriatic-European-Tyrrhenian lithosphere system based on high-quality P wave arrival times. *J. Geophys. Res. Solid Earth* **114**, 5641 (2009).
26. Scafidi, D., Solarino, S. & Eva, C. P wave seismic velocity and Vp/Vs ratio beneath the Italian peninsula from local earthquake tomography. *Tectonophysics* **465**, 1–23 (2009).
27. Molinari, I., Verbeke, J., Boschi, L., Kissling, E. & Morelli, A. Italian and Alpine three-dimensional crustal structure imaged by ambient-noise surface-wave dispersion. *Geochem. Geophys. Geosyst.* **16**, 4405–4421 (2015).
28. Menichelli, I., De Gori, P., Lucente, F. P., Improta, L. & Chiarabba, C. Lithosphere structure, processes, and physical state of the Alpine-Apennine system. *J. Geophys. Res. Solid Earth* **128**, 1–17 (2023).
29. Vanorio, T. et al. The deep structure of the Larderello-Travale geothermal field from 3D microearthquake traveltime tomography. *Geophys. Res. Lett.* **31**, 2–5 (2004).
30. Shapiro, N. M., Campillo, M., Stehly, L. & Ritzwoller, M. H. High-resolution surface-wave tomography from ambient seismic noise. *Science* **307**, 1615–1618 (2005).
31. Lin, F. C., Moschetti, M. P. & Ritzwoller, M. H. Surface wave tomography of the western United States from ambient seismic noise: Rayleigh and Love wave phase velocity maps. *Geophys. J. Int.* **173**, 281–298 (2008).
32. Shapiro, N. M. & Campillo, M. Emergence of broadband Rayleigh waves from correlations of the ambient seismic noise. *Geophys. Res. Lett.* **31**, 2–5 (2004).
33. Tarantola, A. & Valette, B. Modern equipment for narrow fabric weaving and braiding. *Rev. Geophys. Space Phys.* **20**, 219–232 (1982).
34. Bodin, T. et al. Transdimensional inversion of receiver functions and surface wave dispersion. *J. Geophys. Res. Solid Earth* **117**, 1–24 (2012).
35. Dreiling, J. & Tilmann, F. BayHunter - McMC transdimensional Bayesian inversion of receiver functions and surface wave dispersion. (GFZ Data Services, 2019).
36. Dini, A. Ore deposits, industrial minerals and geothermal resources. *Periodico di Mineralogia* **72**, 41–52 (2003).
37. Dini, A., Rielli, A., Di Giuseppe, P., Ruggieri, G. & Boschi, C. The ophiolite-hosted cu-zn vms deposits of tuscany (italy). *Minerals* **14**, 273 (2024).
38. Liotta, D. & Brogi, A. Pliocene-Quaternary fault kinematics in the Larderello geothermal area (Italy): insights for the interpretation of the present stress field. *Geothermics* **83**, 101714 (2020).
39. Serri, G., Innocenti, F. & Manetti, P. Geochemical and petrological evidence of the subduction of delaminated Adriatic continental lithosphere in the genesis of the Neogene-Quaternary magmatism of central Italy. *Tectonophysics* **223**, 117–147 (1993).
40. Piana Agostinetti, N. et al. Discovering geothermal supercritical fluids: A new frontier for seismic exploration. *Sci. Rep.* **7**, 1–9 (2017).
41. Cameli, G., Dini, I. & Liotta, D. Upper crustal structure of the Larderello geothermal field as a feature of post-collisional extensional tectonics (southern Tuscany, Italy). *Tectonophysics* **224**, 413–423 (1993).
42. Bertani, R. et al. The first results of the DESCRAMBLE Project. *Proc. 43rd Workshop Geotherm. Reserv. Eng.* **4**, 1–16 (2018).
43. Driesner, T. & Heinrich, C. A. The system h2o–nacl. part i: Correlation formulae for phase relations in temperature–pressure–composition space from 0 to 1000 c, 0 to 5000 bar, and 0 to 1 xnacl. *Geochimica et. Cosmochimica Acta*. **71**, 4880–4901 (2007).
44. Foley, J. E., Toksoz, M. N. & Batini, F. Inversion of teleseismic travel time residuals for velocity structure in the larderello geothermal field, italy. *Geophys. Res. Lett.* **19**, 5–8 (1992).
45. Stankiewicz, J., Ryberg, T., Haberland, C., Fauzi & Natawidjaja, D. Lake toba volcano magma chamber imaged by ambient seismic noise tomography. *Geophys. Res. Lett.* **37**, 044211 (2010).
46. Chu, R., Helmberger, D. V., Sun, D., Jackson, J. M. & Zhu, L. Mushy magma beneath Yellowstone. *Geophys. Res. Lett.* **37**, 041656 (2010).
47. Paulatto, M. et al. Advances in seismic imaging of magma and crystal mush. *Front. Earth Sci.* **10**, 970131 (2022).
48. Riel, N., Kaus, B. J., Green, E. & Berlie, N. Magemin, an efficient gibbs energy minimizer: application to igneous systems. *Geochem. Geophys. Geosyst.* **23**, e2022GC010427 (2022).
49. Huang, X. & Tong, P. New insight into the velocity and anisotropy structures of the subduction zone in northern sumatra. *Tectonophysics* **892**, 230534 (2024).
50. West, M., Menke, W., Tolstoy, M., Webb, S. & Sohn, R. Magma storage beneath Axial volcano on the Juan de Fuca mid-ocean ridge. *Nature* **413**, 833–836 (2001).
51. Waite, G. P. & Moran, S. C. VP Structure of Mount St. Helens, Washington, USA, imaged with local earthquake tomography. *J. Volcanol. Geotherm. Res.* **182**, 113–122 (2009).
52. Mitchell, M. A., White, R. S., Roecker, S. & Greenfield, T. Tomographic image of melt storage beneath Askja Volcano, Iceland using local microseismicity. *Geophys. Res. Lett.* **40**, 5040–5046 (2013).

53. Wilgus, J., Schmandt, B., Maguire, R., Jiang, C. & Chaput, J. Shear Velocity Evidence of Upper Crustal Magma Storage Beneath Valles Caldera. *Geophys. Res. Lett.* **50**, 1–10 (2023).
54. Lanari, R. et al. Topographic signature of magmatic emplacement at depth: the case of the Larderello-Travale geothermal area (northern Apennines, Italy). *Earth Planet. Sci. Lett.* **659**, 119290 (2025).
55. Barker, S. J. et al. Taupō: an overview of New Zealand's youngest supervolcano. *N.Z. J. Geol. Geophys.* **64**, 320–346 (2021).
56. Biondi, E., Zhu, W., Li, J., Williams, E. F. & Zhan, Z. An upper-crust lid over the Long Valley magma chamber. *Tech. Rep*. https://www.science.org (2023).
57. Principe, C., Vezzoli, L. & La Felice, S. Geology of the Pleistocene volcano of Monte Amiata (southern Tuscany, Italy). *J. Maps* **20**, 2360749 (2024).
58. Gianelli, G. A comparative analysis of the geothermal fields of Larderello and mt. amiata, italy. *Geothermal energy research trends,* 59–85 (Nova Science Publishers, 2008).
59. Giordano, G. & Caricchi, L. Determining the state of activity of transcrustal magmatic systems and their volcanoes. *Annu. Rev. Earth Planet. Sci.* **50**, 231–259 (2022).
60. Chesner, C. A. The Toba Caldera complex. *Quat. Int.* **258**, 5–18 (2012).
61. Barker, S. J., Wilson, C. J., Allan, A. S. & Schipper, C. I. Fine-scale temporal recovery, reconstruction and evolution of a post-supereruption magmatic system. *Contributions Mineral. Petrol.* **170**, 2–40 (2015).
62. Bibby, H. M., Caldwell, T. G., Davey, F. J. & Webb, T. H. Geophysical evidence on the structure of the Taupo Volcanic Zone and its hydrothermal circulation. Tech. Rep. (Springer, 1995).
63. Otway, P. M., Illsley-Kemp, F. & Mestel, E. R. Taupō volcano's restless nature revealed by 42 years of deformation surveys, 1979–2021. *N.Z. J. Geol. Geophys.* **67**, 3–19 (2024).
64. Wilson, C. J. The 26.5 ka Oruanui eruption, New Zealand: an introduction and overview. *J. Volcanol. Geotherm. Res.* **112**, 133–174 (2001).
65. Hurwitz, S., Farrar, C. D. & Williams, C. F. The thermal regime in the resurgent dome of Long Valley Caldera, California: inferences from precision temperature logs in deep wells. *J. Volcanol. Geotherm. Res.* **198**, 233–240 (2010).
66. Tizzani, P. et al. Uplift and magma intrusion at Long Valley caldera from InSAR and gravity measurements. *Geology*. **37**, 63–66 (2009).
67. Hildreth, W. & Wilson, C. J. Compositional zoning of the bishop tuff. *J. Petrol.* **48**, 951–999 (2007).
68. DeNosaquo, K. R., Smith, R. B. & Lowry, A. R. Density and lithospheric strength models of the Yellowstone-Snake River Plain volcanic system from gravity and heat flow data. *J. Volcanol. Geotherm. Res.* **188**, 108–127 (2009).
69. Chang, W.-L., Smith, R. B., Wicks, C., Farrell, J. M. & Puskas, C. M. Accelerated Uplift and Magmatic Intrusion of the Yellowstone Caldera, 2004 to 2006. *Science* **318**, 952–956 (2007).
70. Christiansen, R. L. The quaternary and pliocene Yellowstone Plateau volcanic field of Wyoming, Idaho, and Montana. Tech. Rep., US Department of the Interior, (US Geological Survey, 2001).
71. Romano, V., Tammaro, U. & Capuano, P. A 2-D FEM thermal model to simulate water flow in a porous media: Campi Flegrei caldera case study. *Nonlinear Process. Geophys.* **19**, 323–333 (2012).
72. De Natale, G. et al. The Campi Flegrei caldera: unrest mechanisms and hazards. *Geol. Soc., Lond., Spec. Publ.* **269**, 25–45 (2006).
73. Liotta, D. et al. The progress of geothermal knowledge at Larderello, Italy. *Ital. J. Geosci.* **144**, 228–249 (2025).

Acknowledgements

R. Lanari, K. Michailos, D. Stumpp, S. Papeschi and J. Porras are supported by the Swiss National Science Foundation Sinergia project MIGRATE - A Multidisciplinary and InteGRated Approach for geoThermal Exploration (Grant number: 209434). The salary of Iván Cabrera-Pérez is funded by the European Union's Horizon Europe research and innovation program under the Marie Skłodowska-Curie Postdoctoral Fellowships - Global Fellowships (Grant Agreement No. 101208027, project VERNE).The work was facilitated by the use of the UNIGE High-Performance Computing facilities. We are grateful to Dr. Matteo Roverato, Michele d'Ambrosio and Nicola Piana Agostinetti for helping with the TEMPEST network deployment and data collection. We thank Karen Nicollet for the initial data curation of the TEMPEST seismic data. We acknowledge receiving instruments from the GIPP pool of Potsdam, https://www.gfz.de/sektion/geophysikalische-abbildung-des-untergrunds/infrastruktur/geophysikalischer-geraetepool-potsdam-gipp. We would like to thank two anonymous Reviewers and Kasper van Wijk for the important suggestions that very much helped improving the study. We also would like to thank the private owners who hosted our stations for the experiment. In particular, Dr. Carolina Megale, Fabio Biagini (Formiche di Grosseto), Vincenzo (Hotel Belmare), Tenuta le Ripalte (Lavinia Fusi), Pianosa CNR Research Base, Ernello Armellini (Pienza), Marisa Boschi (Montespertoli), Ricardo Caselli (Firenze), Laura Tonelli (Parco Regionale della Maremma).

Author contributions

M.L. and D.M. conceived the study and M.L. wrote the study. K.M. performed the first tomography analysis and partially wrote the first version of the study. D.S. and I.C.P. run the final inversion and G.e.S., I.C.P., and E.A.J.B. supported the early tomography analysis. D.M., E.A.J.B., G.i.S., R.M., C.D.V., M.B., J.P.L., F.M.B., D.P., and M.L. took part in the deployment of the TEMPEST network. R.L., S.P., F.F., and J.S. contributed to develop concepts and foster observations. All authors reviewed the manuscript.

Competing interests

The authors declare no competing interests.

Additional information

Supplementary information The online version contains supplementary material available at https://doi.org/10.1038/s43247-026-03334-0.

Correspondence and requests for materials should be addressed to Matteo Lupi or Iván Cabrera-Pérez.

Peer review information *Communications Earth and Environment* thanks Kasper van Wijk and the other, anonymous, reviewer(s) for their contribution to the peer review of this work. Primary Handling Editor: Alireza Bahadori. A peer review file is available.